Astron. Nachr. / AN **333**, No. 10, 1040 – 1043 (2012) / **DOI** 10.1002/asna.201211825

Acoustic glitches in solar-type stars from *Kepler*

A. Mazumdar[1,⋆], **M.J.P.F.G. Monteiro**[2,3], **J. Ballot**[4,5], **H.M. Antia**[6], **S. Basu**[7], **G. Houdek**[8,9], **S. Mathur**[10], **M.S. Cunha**[2], **V. Silva Aguirre**[8,11], **R.A. García**[12], **D. Salabert**[13], **G.A. Verner**[14], **J. Christensen-Dalsgaard**[8], **T.S. Metcalfe**[15], and **W.J. Chaplin**[14]

[1] Homi Bhabha Centre for Science Education, TIFR, V. N. Purav Marg, Mankhurd, Mumbai 400088, India
[2] Centro de Astrofísica da Universidade do Porto, Rua das Estrelas, 4150-762 Porto, Portugal
[3] Departamento de Física e Astronomia, Faculdade de Ciências da Universidade do Porto, Rua do Campo Alegre, 4169-007 Porto, Portugal
[4] CNRS, Institut de Recherche en Astrophysique et Planétologie, 14 avenue Edouard Belin, 31400 Toulouse, France
[5] Université de Toulouse, UPS-OMP, IRAP, 31400 Toulouse, France
[6] Tata Institute of Fundamental Research, Homi Bhabha Road, Mumbai 400005, India
[7] Astronomy Department, Yale University, P.O. Box 208101, New Haven, CT 065208101, USA
[8] Stellar Astrophysics Centre, Department of Physics and Astronomy, Aarhus University, Ny Munkegade 120, DK-8000 Aarhus C, Denmark
[9] Institute of Astronomy, University of Vienna, 1180, Vienna, Austria
[10] High Altitude Observatory, NCAR, P.O. Box 3000, Boulder, CO 80307, USA
[11] Max-Planck-Institut für Astrophysik, Karl-Schwarzschild-Str. 1, D-85748 Garching, Germany
[12] Laboratoire AIM, CEA/DSM, CNRS, Université Paris Diderot, IRFU/SAp, Centre de Saclay, 91191 Gif-sur-Yvette Cedex, France
[13] Laboratoire Lagrange, UMR7293, Université de Nice Sophia-Antipolis, CNRS, Observatoire de la Côte d'Azur, 06304 Nice, France
[14] School of Physics and Astronomy, University of Birmingham, Edgbaston, Birmingham, B15 2TT, UK
[15] Space Science Institute, Boulder, CO 80301, USA

Received 2012 Oct 26, accepted 2012 Nov 7
Published online 2012 Dec 3

Key words stars: interiors – stars: oscillations

We report the measurement of the acoustic locations of layers of sharp variation in sound speed in the interiors of 19 solar-type stars observed by the *Kepler* mission. The oscillatory signal in the frequencies arising due to the acoustic glitches at the base of the convection zone and the second helium ionisation zone was utilised to determine their location by four independent methods. Despite the significantly different methods of analysis, remarkable agreement was found between the results of these four methods. Further, the extracted locations of these layers were found to be consistent with representative models of the stars.

1 Introduction

An acoustic glitch in a star is a region where the sound speed undergoes an abrupt variation due to sharp change in the structure. Such a glitch introduces an oscillatory component in the eigenfrequencies of the star proportional to $\sin(4\pi\tau_{\rm g}\nu_{n,l}+\phi)$ (Gough 1990; Vorontsov 1988), where $\tau_{\rm g}=\int_{r_{\rm g}}^{R_{\rm s}}{\rm d}r/c$ is the acoustic depth of the glitch measured from the surface, c the adiabatic speed of sound, $r_{\rm g}$ the radial distance of the glitch, $R_{\rm s}$ the seismic radius of the star, $\nu_{n,l}$ the frequency of a mode with radial order n and degree l, and ϕ a phase factor. Each glitch causes an oscillatory signal with a "periodicity" of the corresponding acoustic depth.

The major acoustic glitches in solar-type stars are the boundaries between radiative and convective regions, especially the base of the outer convection zone (hereafter referred to as BCZ) and the layers of ionisation of elements, especially helium (hereafter HeIIZ for the He II ionisation region). The acoustic radii (measured from the centre) of the two glitches due to the BCZ and HeIIZ are defined as $T_{\rm BCZ}=\int_0^{r_{\rm BCZ}}{\rm d}r/c$, $T_{\rm HeIIZ}=\int_0^{r_{\rm HeIIZ}}{\rm d}r/c$, where $r_{\rm BCZ}$ and $r_{\rm HeIIZ}$ are the radial positions of the glitches. In particular, the radial position of the local minimum of the adiabatic index $\gamma_1=(\partial\ln p/\partial\ln\rho)_s$ (p and ρ are pressure and density respectively and s is specific entropy) in the He II region is taken to be $r_{\rm HeIIZ}$. The acoustic depths (measured from the surface) for BCZ and HeIIZ are $\tau_{\rm BCZ}$ and $\tau_{\rm HeIIZ}$, respectively, defined as $\tau_{\rm BCZ}=\int_{r_{\rm BCZ}}^{R_{\rm s}}{\rm d}r/c\equiv T_0-T_{\rm BCZ}$, $\tau_{\rm HeIIZ}=\int_{r_{\rm HeIIZ}}^{R_{\rm s}}{\rm d}r/c\equiv T_0-T_{\rm HeIIZ}$. Here T_0 is the total acoustic radius of the star, which can be calculated as $T_0=\int_0^{R_{\rm s}}{\rm d}r/c$, where $R_{\rm s}$ is the seismic radius of the star, which may be considered as a fiducial radius that defines the outer phase of the acoustic modes.

⋆ Corresponding author: anwesh@tifr.res.in

In the present work we determined the acoustic locations of the BCZ and HeIIZ in 19 solar-like stars observed by the *Kepler* mission (Borucki et al. 2010; Koch et al. 2010) during 9 months. The frequencies of these stars are adopted from Appourchaux et al. (2012).

2 Methods

We used four independent methods (labelled A to D) that employ different techniques to determine the acoustic depths or radii of the major glitches from their oscillatory signals in the frequencies.

2.1 Method A

In this method, the oscillatory signal in the frequencies are fitted separately to two components corresponding to BCZ and HeIIZ, after removing a smooth trend. The fitting procedure used is similar to that described by Monteiro et al. (2000). The smooth component is fitted iteratively by polynomials to frequencies of different degrees separately and subsequently the residuals are fitted to the BCZ and HeIIZ glitch signals, $\delta\nu_{\rm BCZ}$ and $\delta\nu_{\rm HeIIZ}$, respectively, described by the functions

$$\delta\nu_{\rm BCZ} \simeq A_{\rm BCZ}\left(\frac{\nu_r}{\nu}\right)^2 \cos(4\pi\tau_{\rm BCZ}\nu + 2\phi_{\rm BCZ})\,, \qquad (1)$$

$$\delta\nu_{\rm HeIIZ} \simeq A_{\rm HeIIZ}\left(\frac{\nu_r}{\nu}\right)\sin^2(2\pi\beta_{\rm HeIIZ}\,\nu)\times \cos(4\pi\tau_{\rm HeIIZ}\nu + 2\phi_{\rm HeIIZ})\,. \qquad (2)$$

Such fits for one typical *Kepler* star are shown in the first panel of Fig. 1.

There are seven free parameters in these expressions: $A_{\rm BCZ}$, $\tau_{\rm BCZ}$, $\phi_{\rm BCZ}$, $A_{\rm HeIIZ}$, $\beta_{\rm HeIIZ}$, $\tau_{\rm HeIIZ}$, and $\phi_{\rm HeIIZ}$. In addition there are typically three parameters used in removing the smooth component. Uncertainties on these parameters were estimated through Monte Carlo simulations.

2.2 Method B

This method involves the second differences of the frequencies (defined as $\Delta_2\nu(n,l) = \nu(n-1,l) - 2\nu(n,l) + \nu(n+1,l)$) to determine $\tau_{\rm BCZ}$ and $\tau_{\rm HeIIZ}$ simultaneously by fitting the functional form adapted from Houdek & Gough (2007) (Eq. (22) therein) to the oscillatory signals

$$\Delta_2\nu = a_0 + (b_2/\nu^2)\sin(4\pi\nu\tau_{\rm BCZ} + 2\phi_{\rm BCZ}) + [c_0\nu\exp(-c_2\nu^2)]\sin(4\pi\nu\tau_{\rm HeIIZ} + 2\phi_{\rm HeIIZ}), \qquad (3)$$

where a_0, b_2, c_0, c_2, $\tau_{\rm BCZ}$, $\phi_{\rm BCZ}$, $\tau_{\rm HeIIZ}$ and $\phi_{\rm HeIIZ}$ are 8 free parameters of fitting. The fitting procedure is similar to the one described by Mazumdar et al. (2012). The fit is carried out through a nonlinear χ^2 minimisation, weighted by the errors in the data. The correlation of errors in the second differences is accounted for by defining the χ^2 using a covariance matrix. The effects of the errors are considered by repeating the fit for 1000 realisations of the data, produced by skewing the frequencies by random errors corresponding to a normal distribution with standard deviation equal to the quoted 1σ error in the frequencies. The median value of each parameter for 1000 realisations is taken as its fitted value. The $\pm1\sigma$ error in the parameter is estimated from the range of values covering 34 % area on each side of the median in the histogram of fitted values. Thus the quoted errors in these parameters reflect the width of these histograms on two sides of the median value. The best fit to $\Delta_2\nu$ and the histograms for $\tau_{\rm BCZ}$ and $\tau_{\rm HeIIZ}$ are shown in the second panel of Fig. 1 for one typical star.

2.3 Method C

Here we adopt the method proposed by Houdek & Gough (2007, 2011) who derived approximate expressions for the frequency contributions $\delta\nu_i$ arising from acoustic glitches in solar-type stars. The complete expression for the frequency contributions is

$$\delta\nu_i = \delta_\gamma\nu_i + \delta_{\rm c}\nu_i + \delta_{\rm u}\nu_i\,, \qquad (4)$$

where the terms on the RHS are the individual acoustic glitch components localised at different depths inside the star (see Houdek & Gough (2007, 2011) for detailed expressions).

The first component, $\delta_\gamma\nu$, arises from the variation in γ_1 induced by helium ionisation. The effects of both the first and second helium ionisation are taken into consideration. The second component in Eq. (4), $\delta_{\rm c}\nu$ arises from the acoustic glitch at the base of the convection zone resulting from a near discontinuity in the second derivative of density. We model this acoustic glitch with a discontinuity in the squared acoustic cutoff frequency at $\tau_{\rm BCZ}$ coupled with an exponential relaxation in the radiative zone beneath, with acoustical scale time $\tau_0 = 80\,$s.

The third component $\delta_{\rm u}\nu_i$ is produced, in part, by wave refraction in the stellar core by the ionisation of hydrogen and by the upper superadiabatic boundary layer of the envelope convection zone. Since it is difficult to model we approximate it as a series of inverse powers of ν, truncated at the cubic order.

There are eleven coefficients in the detailed expressions for the three components in Eq. (4), including $\tau_{\rm BCZ}$ and $\tau_{\rm HeIIZ}$, which were found by fitting the second differences of $\delta\nu_i$ to the second differences of the observed frequencies by a non-linear least squares method similar to that described for method B (see third panel of Fig. 1). The covariance matrix of the uncertainties in the fitting coefficients were established by Monte Carlo simulation.

2.4 Method D

In this method we exploit the oscillatory signature of the glitches in the 3-point differences
$d_{01,n} = \frac{1}{2}(2\nu_{n,0} - \nu_{n-1,1} - \nu_{n,1})$,
$d_{10,n} = -\frac{1}{2}(2\nu_{n,1} - \nu_{n,0} - \nu_{n+1,0})$,

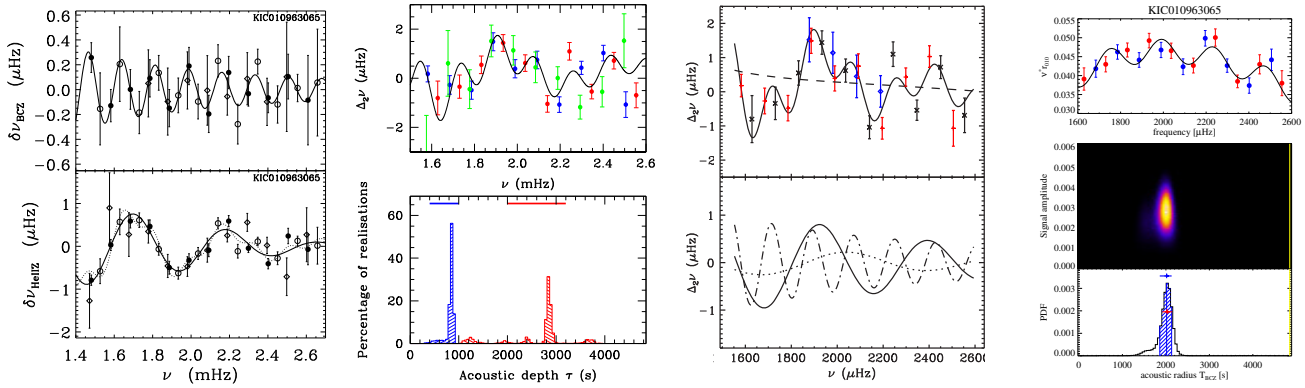

Fig. 1 (online colour at: www.an-journal.org) Results for one typical *Kepler* star, KIC 010963065, are shown for all the four methods as illustration. The four panels correspond to the methods A to D, arranged from left to right. *First panel* (Method A): fits (solid lines) of the Eqs. (1) (*upper graph*) and (2) (*lower graph*) to the residuals of frequencies after removing a smooth component iteratively. The points correspond to $l = 0$ (black circles), $l = 1$ (open circles) and $l = 2$ (diamonds). *Second panel* (Method B): fit of Eq. (3) (black curve) to second differences of the mean frequencies (blue, red and green for $l = 0, 1, 2$ respectively) (*upper graph*) and the histograms for the fitted values of $\tau_{\rm HeIIZ}$ (blue) and $\tau_{\rm BCZ}$ (red) for different realisations of the data (*lower graph*). *Third panel* (Method C): fit to second differences (solid curve) based on the analysis by Houdek & Gough (2007, 2011) and the smooth contribution (dashed curve) are shown in the *upper graph*. The *lower graph* displays the remaining individual contributions from the acoustic glitches to second differences: the dotted and solid curves are the contributions from the He I and He II ionisation, respectively, and the dot-dashed curve is the contribution from the BCZ. *Fourth panel* (Method D): determination of $T_{\rm BCZ}$ using frequency ratios. *Top graph* shows observed $\nu^* r_{010}$ (blue and red dots for $l = 0$ and 1, respectively) and the best MCMC fit to Eq. (5) (solid line). *Middle graph* is the 2-D probability function in the plane (T, A). *Bottom graph* shows marginal probability distributions for the parameter T with median value indicated by vertical blue line and hatched area shows the 68 %-level confidence interval.

and the corresponding ratios

$r_{01,n} = d_{01,n}/\Delta\nu_{1,n}$, $r_{10,n} = d_{10,n}/\Delta\nu_{0,n+1}$.

We denote by d_{010} and r_{010} the sets $\{d_{01}, d_{10}\}$ and $\{r_{01}, r_{10}\}$, respectively.

The effects of the outer layers are mostly removed in these variables but the most internal glitches, such as the BCZ, imprint their signatures over the global trend. Roxburgh (2009) showed that we can determine the solar $T_{\rm BCZ}$ by using Fourier transform on the residuals obtained after removing the global trend from the solar frequency separation ratios. However, information about surface layers, including He I and He II ionisation zones, are lost in these variables.

We developed a pipeline to determine $T_{\rm BCZ}$ from $l = 0$ and 1 modes. Instead of a Fourier transform on the detrended data, we fit the variable $y = \nu^* r_{010}$ (or $y = \nu^* d_{010}$) with the following expression representing both the smooth trend and the oscillatory components

$$f(\nu) = \sum_{k=0}^{m} \frac{c_k}{(\nu + \nu_{\rm r})^k} + A\sin(4\pi T\nu + \phi), \qquad (5)$$

where $\nu^* = \nu/\nu_{\rm r}$ and $\nu_{\rm r}$ is a reference frequency. We have $m + 3$ free parameters: $\{c_k\}$, A, T, and ϕ.

To estimate uncertainties for $T_{\rm BCZ}$ we employed a Markov Chain Monte Carlo (MCMC) fitting algorithm similar to the ones described in Benomar et al. (2009) and Handberg & Campante (2011). We used uniform priors for A, T, and ϕ. The priors for $\{c_k\}$ are uniform over $[\tilde{c}_k - 3\sigma_k, \tilde{c}_k + 3\sigma_k]$ with Gaussian decay, where $\tilde{c}_k$ and σ_k are the mean and standard deviation of c_k obtained from a purely linear fit. The MCMC was run for 10^7 iterations.

Posterior probability distribution function (PDF) for T is plotted for the example star KIC010963065 in the fourth panel of Fig. 1. Usually the PDFs exhibit a unique and clear mode that we attribute to the BCZ. $T_{\rm BCZ}$ was then estimated as the median of the distribution and 1σ error bars were taken as 68 % confidence limit of the PDF. Some other PDFs exhibit other small peaks which may be due to noise or possibly due to other glitch signatures present in the data. This method has been successful mainly for main-sequence stars, but not so much for subgiant stars with mixed modes.

3 Results

We find, in general, excellent agreement between the results obtained through the four methods described above. In most cases the $\tau_{\rm BCZ}$ (or the corresponding $T_{\rm BCZ}$) agree with each other well within respective 1σ error bars. In terms of relative uncertainties, the $\tau_{\rm BCZ}$ and $\tau_{\rm HeIIZ}$ values from different methods agree pairwise within 10 % and 5 %, respectively for most of the stars. In Fig. 1 we illustrate the results from the four methods A to D for one typical star, KIC 010963065.

As a sanity check on the values of the acoustic radii of the acoustic glitches determined from the observed frequencies of a star, we also compared them with theoretical model values. For each star, a large number of representative models were constructed and the same method was applied for the theoretical frequencies of these as was done for the observed frequencies. The details of the models can be found in Basu et al. (2010). We also compared our results

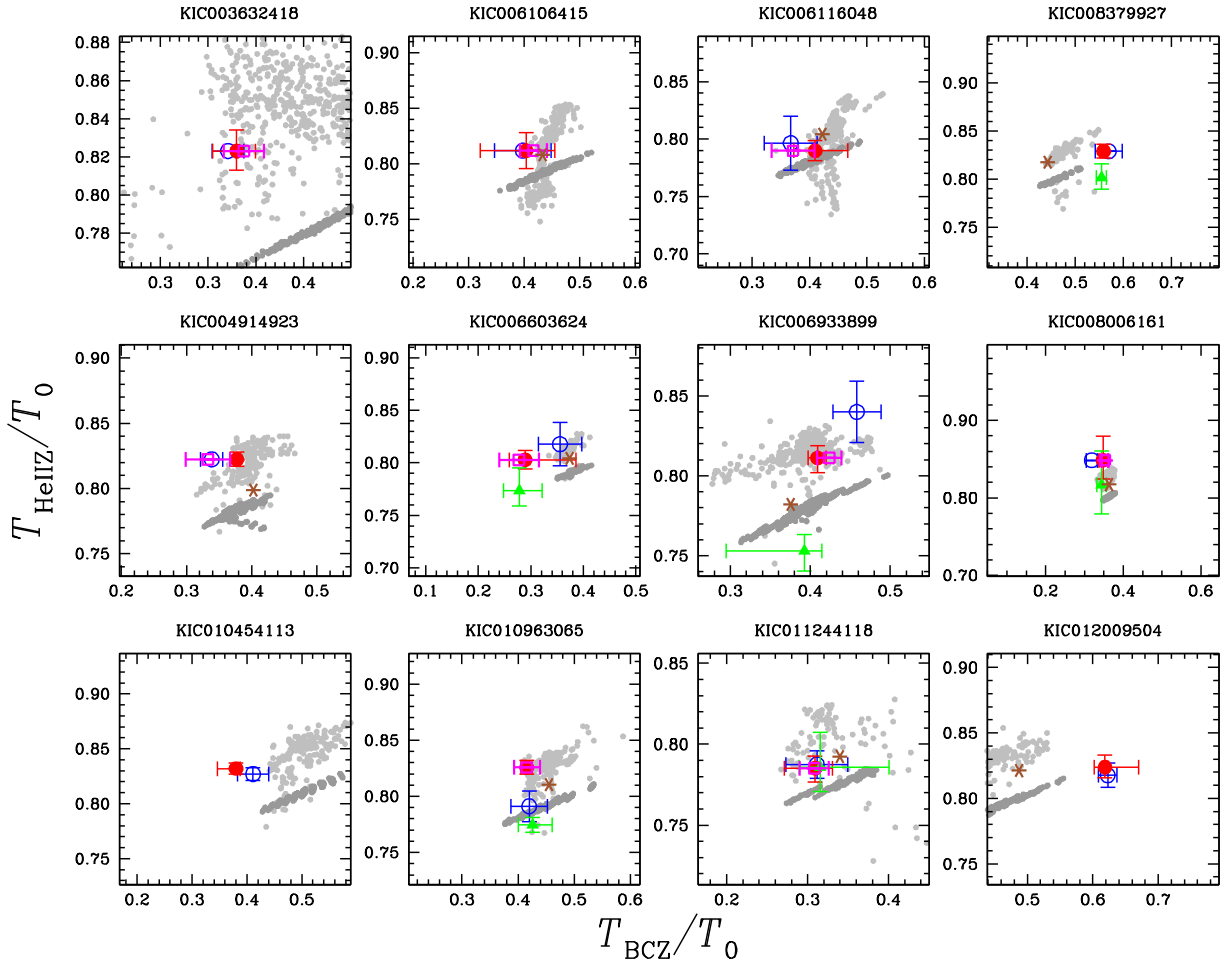

Fig. 2 (online colour at: www.an-journal.org) Comparison of fractional acoustic radii $T_{\rm BCZ}/T_0$ and $T_{\rm HeIIZ}/T_0$ determined from the oscillatory signal in the *Kepler* frequencies of 12 stars by up to four methods (blue empty circle for A, red filled circle for B, green filled triangle for C and magenta empty square for D, each with error bars) with corresponding values from representative models of the stars. For method A, in cases where $\tau_{\rm HeIIZ}$ was not determined, and for all cases for method D, the $\tau_{\rm HeIIZ}$ value has been provided by the one determined by method B. The dark grey circles indicate the actual value of the fractional acoustic radii in the stellar models, while the light grey dots represent the values of the fractional acoustic radii determined from the theoretical frequencies of the models by method B. The brown asterisk indicates the AMP model.

with those in an optimally fitted model of each star obtained through the Asteroseismic Modeling Portal (AMP, Metcalfe et al. 2009; see Mathur et al. 2012) for further details of these stars). For most of the stars the estimated location of the glitches were found to be in close agreement with the model values, within error bars (see Fig. 2).

The present work demonstrates the viability of the techniques applied to determine the acoustic location of layers of sharp variation of sound speed in the stellar interior.

References

Appourchaux, T., Chaplin, W.J., García, R.A., et al.: 2012, A&A 543, A54

Basu, S., Chaplin, W.J., Elsworth, Y.: 2010, ApJ 710, 1596

Benomar, O., Appourchaux, T., Baudin, F.: 2009, A&A 506, 15

Borucki, W.J. et al.: 2010, Sci 327, 977

Cunha, M.S., Brandão, I.M.: 2011, A&A 529, A10

Gough, D.O.: 1990, Progress of Seismology of the Sun and Stars 367, 283

Handberg, R., Campante, T.L.: 2011, A&A 527, A56

Houdek, G., Gough, D.O.: 2007, MNRAS 375, 861

Houdek, G., Gough, D.O.: 2011, MNRAS 418, 1217

Koch, D.G., et al.: 2010, ApJ 713, L79

Mathur, S., Metcalfe, T.S., Woitaszek, M., et al.: 2012, ApJ 749, 152

Mazumdar, A., Michel, E., Antia, H.M., Deheuvels, S.: 2012, A&A 540, A31

Metcalfe, T.S., Creevey, O.L., Christensen-Dalsgaard, J.: 2009, ApJ 699, 373

Monteiro, M.J.P.F.G., Christensen-Dalsgaard, J., Thompson, M.J.: 2000, MNRAS 316, 165

Roxburgh, I.W.: 2009, A&A 493, 185

Vorontsov, S.V.: 1988, in: J. Christensen-Dalsgaard, S. Fransden (eds.), *Advances in helio- and asteroseismology*, IAU Symp. 123, p. 151